

# Read Mapping Near Non-Volatile Memory

S. Karen Khatamifard\* Zamshed Chowdhury\* Nakul Pande\* Meisam Razaviyayn†  
Chris Kim\* Ulya R. Karpuzcu\*

\* University of Minnesota † University of Southern California

\* {khatami, chowh005, nakul, chriskim, ukarpuzc}@umn.edu † razaviya@usc.edu

## ABSTRACT

DNA sequencing is the physical/biochemical process of identifying the location of the four bases (Adenine, Guanine, Cytosine, Thymine) in a DNA strand. As semiconductor technology revolutionized computing, modern DNA sequencing technology (termed Next Generation Sequencing, NGS) revolutionized genomic research. As a result, modern NGS platforms can sequence hundreds of millions of short DNA fragments in parallel. The sequenced DNA fragments, representing the output of NGS platforms, are termed *reads*. Besides genomic variations, NGS imperfections induce noise in *reads*. Mapping each *read* to (the most similar portion of) a reference genome of the same species, i.e., *read mapping*, is a common critical first step in a diverse set of emerging bioinformatics applications. Mapping represents a search-heavy memory-intensive similarity matching problem, therefore, can greatly benefit from near-memory processing. Intuition suggests using fast associative search enabled by Ternary Content Addressable Memory (TCAM) by construction. However, the excessive energy consumption and lack of support for similarity matching (under NGS and genomic variation induced noise) renders direct application of TCAM infeasible, irrespective of volatility, where only *non-volatile* TCAM can accommodate the large memory footprint in an area-efficient way. This paper introduces GeNVVoM, a scalable, energy-efficient and high-throughput solution. Instead of optimizing an algorithm developed for general-purpose computers or GPUs, GeNVVoM rethinks the algorithm and non-volatile TCAM-based accelerator design together from the ground up. Thereby GeNVVoM can improve the throughput by up to  $113.5\times$  ( $3.6\times$ ); the energy consumption, by up to  $210.9\times$  ( $1.36\times$ ), when compared to a GPU (accelerator) baseline, which represents one of the highest-throughput implementations known.

## 1. INTRODUCTION

DNA sequencing is the physical or biochemical process of extracting the order of the four bases (Adenine, Guanine, Cytosine, Thymine) in a DNA strand. As semiconductor technology revolutionized computing, DNA sequencing technology, termed *High-throughput Sequencing* or *Next Generation Sequencing* (NGS), revolutionized genomic research. As a result, modern NGS platforms can sequence hundreds of millions of short DNA fragments in parallel. The sequenced fragments (which represent the NGS output) are referred to as short *reads* and typically contain 100-200 bases [1]. The focus of this paper is *read mapping*, a common critical first

step spanning a rich and diverse set of emerging bioinformatics applications: mapping each NGS *read* to (the most similar portion of) a reference genome of the same species (which itself represents a full-fledged assembly of already processed *reads*).

As a representative example, modern NGS machines from Illumina [1], a prominent NGS platform producer, can sequence more than 600Giga-bases (Gba) per one run,  $200\times$  the length of a human genome of approximately 3Gba, which translates into hundreds of millions of output *reads*. Fig. 1 depicts the scaling trend in terms of the total number of human genomes sequenced. The values until 2015 reflect historical publication records, with milestones explicitly marked. The values beyond 2015 reflect three different projections: the first, following the historical growth until 2015; the second, a more conservative prediction from Illumina; the third, Moore's Law. Historically, the total quantity has been doubling approx. every 7 months. Even the more conservative projections from Fig. 1 (i.e.,  $2\times$  increase every 12 or 18 months) result in a very rapid growth, which challenges the throughput performance of *read mapping*.

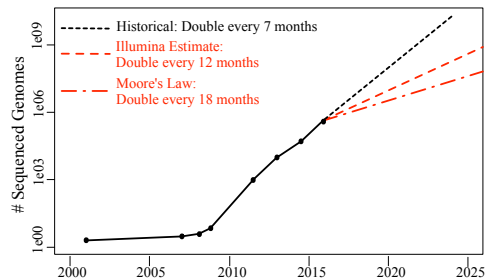


Figure 1: Scaling trend for DNA sequencing [2].

The wildly increasing scale of the problem per Fig. 1 renders well-studied pair-wise similarity detection algorithms inefficient [3]. Worse, *reads* are subject to noise due to imperfections in NGS platforms and genomic variations, which adds to the complexity. Both algorithmic solutions and hardware acceleration via GPUs [4] or FPGAs [5] therefore have to trade mapping accuracy for throughput performance. In other words, *read mapping* by definition is after *similarity matching*. As optimizations are usually confined to compute-intensive stages of mapping, considering scaling projections from Fig. 1, most of these solutions are fundamentally limited by data transfer overheads. In this paper, we instead take a data-centric position to guide the design (and explore the design space) of scalable, energy-efficient and high-throughput *read mapping*. Specifically, instead of optimizing an algorithm developed for general-purpose computers or GPUs, we rethink the algorithm from the ground up along with the

accelerator design.

*Read mapping* represents a search-heavy memory intensive operation and barely requires complex floating point arithmetic, therefore, can greatly benefit from near-memory processing. Intuition suggests using fast parallel associative search, enabled by Ternary Content Addressable Memory (TCAM) by construction, in matching short *read* patterns with portions of the large reference genome (stored in TCAM). As we will explain in Section 2, however, only *non-volatile* TCAM can accommodate the large memory footprint in an area- and energy-efficient manner [6]. Even then, brute-force non-volatile TCAM search over as large of a search space as *read mapping* demands induces excessive energy consumption, rendering (non-volatile) TCAM-based acceleration infeasible. At the same time, by construction, (non-volatile) TCAM cannot handle similarity matching under NGS or genomic variation induced noise.

This paper provides an effective solution, GeNVoM, to tap the potential of *non-volatile* TCAM for scalable, energy-efficient high-throughput *read mapping*. GeNVoM

- introduces a novel similarity matching mechanism for resistive non-volatile TCAM (which can only handle exact matches by construction), to trade mapping accuracy for throughput and energy efficiency in a much more scalable manner than existing solutions;
- features a novel genomic data representation for efficient similarity matching without compromising storage complexity;
- tailors common search space pruning approaches to its novel similarity matching mechanism in order to identify and discard unnecessary non-volatile TCAM accesses (and thereby, to prevent excessive energy consumption);
- accounts for the most prevalent manifestations of noise induced by NGS imperfections and genomic variations during similarity matching, including (base) gaps and insertions/deletions in *reads*;
- employs multi-phase hierarchical similarity matching to enhance mapping accuracy and scalability, where each phase performs progressively more sophisticated mapping, considering only the subset of *reads* the previous phase fails to map.

In the following, we introduce a proof-of-concept GeNVoM implementation. Specifically, Section 2 discusses basics; Section 3 covers implementation details; Sections 4 and 5 detail the evaluation; Section 6 provides a compare and contrast to related work; and Section 7 summarizes our findings.

## 2. GeNVoM: MACROSCOPIC VIEW

**Scope:** Short (i.e., 100-200 base long) *reads* from modern Illumina NGS platforms [1] constitute more than 90% of all *reads* in the world currently. Accordingly, GeNVoM is designed for short *read* mapping.

**Terminology:** Without loss of generality, we will refer to each *read* simply as a *query*; and the reference genome, as the *reference*. Each *query* and the *reference* represent strings of characters from the alphabet {A, G, C, T} which stand for the bases {Adenine, Guanine, Cytosine, Thymine}. The inputs to GeNVoM are a dataset of *queries* and the *reference*, where the *reference* is many orders of magnitude longer than each *query*. For example, if the *reference* is the human genome, *reference* length is approximately  $3 \times 10^9$  bases. On the other hand, technological capabilities of modern NGS platforms limit the maximum *query* length.

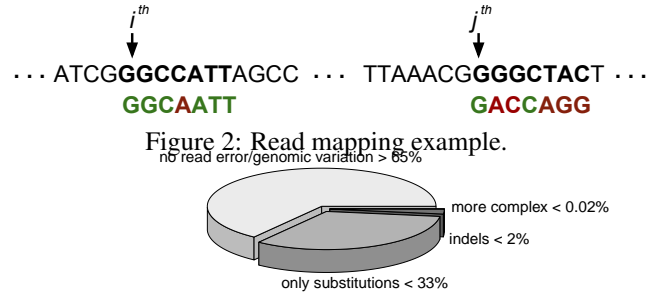


Figure 3: Manifestation of genomic variations & read errors.

### 2.1 Problem Definition: Read Mapping

**Basics:** *Read mapping* entails finding the most *similar* portions of a given *reference* to each *query* from a dataset corresponding to the same species, as output by an NGS machine. Fig. 2 demonstrates an example, with different portions from the same *reference* on top; two sample *queries* to be mapped, at the bottom. The first (second) *query* results in one (five) base-mismatch(es) when aligned to the  $i^{th}$  ( $j^{th}$ ) base of the *reference*. The *query* length is not representative, but simplifies demonstration.

GeNVoM’s input *queries* are subject to noise due to imperfections in NGS platforms and potential genomic variations. Therefore, *read mapping* by definition is after *similarity* rather than an *exact match*. Hence, for each input *query*, GeNVoM tries to locate the *most similar* sub-sequence of the *reference* to the *query*, and returns the range of its indices.

**Mapping Reverse Complement of reads:** It is not uncommon for NGS platforms to sequence DNA strands in reverse direction. This happens when sequencing starts from the last base of a DNA strand. In this case, the platform outputs the reverse complement of a *read* by interchanging A with T, and C with G. For example, the reverse complement of the sequence ACCGCCTA is TAGGCGGT. NGS platforms typically sequence almost half of the DNA strands in reverse order, hence, GeNVoM is designed to handle reverse complements.

**Sources of Noise in Similarity Matching:** In general, the sequenced genome (where the *reads* are coming from) is expected to be slightly different from the *reference* genome, even though they represent the very same species. *Genomic variations* induce such differences, which can lead to base-mismatches between the *queries* and the *reference*, since the *queries* come from the sequenced genome as opposed to the *reference*. NGS platform imperfections, as well, can result in false base-mismatches between the *queries* and the *reference*, due to the so-called *read errors* during sequencing. We will next discuss the most prevalent manifestations of genomic variations and read errors.

**Noise Manifestation:** Most common genomic variations and read errors manifest themselves in three ways: Random *insertion* of a base, random *deletion* of a base, and random *substitution* of a base with another. Insertions and deletions are often referred to as *indels*. The expected rates of indels and substitutions depend on the type of genomes (hence species) and the NGS technology.

As a representative example, Fig. 3 demonstrates the typical share of *reads* having no read errors/genomic variations (>65%), at least one substitution (and no indels) (<33%), at least one indel (<2%), and more complex manifestations (<0.02%) [7, 8, 9, 10]. Mapping under rare complex man-

ifestations (such as long-indels, gaps, base duplications or inversions) is a daunting task, and to date there is no widely-accepted algorithm to cover all [9, 11]. As Fig. 3 shows, substitutions are dominant. Although indel rate is on the lower side, detecting indels is critical for many downstream applications. Hence, GeNVom is designed to cover both substitutions and indels, but optimized for the common case (no read error/genomic variation and only substitutions), which covers more than 98% of the *reads* per Fig. 3. As we will demonstrate in Section 3.4, straight-forward expansion of GeNVom to more complex manifestations such as gaps is also possible.

## 2.2 Why Naive (Non-Volatile) TCAM-based Acceleration Does Not Work

*Read mapping* essentially is a search-heavy memory intensive pattern matching problem. This suggests TCAM-based acceleration, which by construction can support fast parallel in-memory search. TCAM is a special variant of associative memory (which permits data retrieval by indexing by content rather than by address) that can store and search the “don’t care” state X in addition to a logic 0 or 1. Considering the scale of the problem, however, only *non-volatile* TCAM can accommodate the large memory footprint in an area- and energy-efficient manner [6].

We will next look into the energy consumption of *read mapping*, comparing a non-volatile TCAM-based implementation with a highly optimized GPU-based solution deploying one of the fastest known algorithms to date [12]. The non-volatile TCAM mimics the least energy-hungry implementation from Guo et al. [6], corresponding to an array size of  $1K \times 1K$ bits = 1Mbits. For this design point, searching for a pattern of length 1Kbits (which represents the maximum-possible length, i.e., the row length) in the entire array takes approximately 2.5ns and consumes 245nJ.

If we simply encode each base from the alphabet {A, G, C, T} using 2 bits, and if a human genome of approximately 3Giga-bases (= 6Gbits) represents the *reference*, the *reference* can fit into 6K TCAM arrays (of size  $1K \times 1K$ bits = 1Mbits). For each *query* of a typical length of 100 bases [1], i.e., 200 bits, the following naive procedure can cover the entire search space: By construction, each  $1K \times 1K$ bit TCAM array can search for at most one 1Kbit pattern at a time, which resides in a query register. We can align the most significant bit of the (200bit-long) *query* with the most significant bit position of TCAM’s 1Kbit query register, and pad the remaining (1K-200) bits by Xs, for the very first search in the array. We can then repeat the search by shifting the contents of TCAM’s query register (i.e., the padded *query*) to the right by one bit at a time, leaving the unused more significant bit positions with Xs, until the least significant bit of the *query* reaches the least significant bit position in the query register. The total number of these bit-wise shifts (and hence, searches) would be in the order of the row length  $\approx 1K$ . Putting it all together, mapping a given *query* to the *reference* in this case would take around 1K searches in each of the 6K arrays, with 245nJ consumed per search. The overall energy consumption therefore would become  $6K \times 1K \times 245nJ \approx 1500mJ$ .

The GPU solution from Luo et al. [12] on the other hand, can process 133.3K *queries* per second. Hence, it takes 1/133.3K seconds to map a single *query*. Even under the unrealistic assumption (favoring TCAM) that the entire peak average power (TDP) goes to mapping a single *query* to the

*reference*, the energy consumption would become at most  $235W \times (1/133.3K)s \approx 1.8mJ$ .

The GPU and TCAM designs feature similar technology nodes, however, even by favoring TCAM, the TCAM-based naive implementation consumes approx. 3 orders of magnitude more energy than the GPU-based. This difference stems from the gap in the size of the search spaces. While the TCAM-based design considers the entire search space to cover all possible alignments, the GPU-based design first prunes the search space to eliminate infeasible alignments, which in turn leads to orders of magnitude less number of (search) operations. GeNVom, while deploying non-volatile TCAM arrays, adopts a similar pruning strategy to enable more energy-efficient search.

Even if excessive energy consumption was not the case, (non-volatile) TCAM has another fundamental limitation which hinders applicability to *read mapping*. As we will detail in Section 3.3, even in the presence of “don’t cares”, TCAM cannot handle similarity matching considering various manifestations of noise due to NGS errors and genomic variations (Section 2.1).

To summarize, both, *the excessive energy consumption and lack of support for similarity matching render a direct adaptation of non-volatile TCAM-based search infeasible*. The energy overhead of conventional volatile TCAM would be even higher [6], while the restriction on similarity matching directly applies irrespective of volatility.

GeNVom unlocks the throughput potential of non-volatile TCAM in a scalable and energy-efficient manner through

- a novel **non-volatile** resistive TCAM design capable of **similarity matching** (Sect. 3.3);
- a novel **genomic data representation for similarity matching** without compromising storage complexity (Sect. 3.2);
- a common filtering mechanism [13] for **search space pruning adapted to non-volatile similarity matching** to prevent excessive energy consumption (Sect. 3.1);
- **hierarchical similarity matching** to maximize mapping accuracy without compromising scalability (Section 3.4).

Designed for similarity search (in the presence of NGS or genomic variation triggered noise), GeNVom’s non-volatile TCAM arrays can directly handle substitutions, by construction (Sect. 3.3). To cover indels and more complex corruptions, on the other hand, GeNVom adapts *anchoring* within its multi-phase mapping hierarchy (Sect. 3.4). The key insight is that complex corruptions that can lead to failed mappings are much less likely to occur in *all* portions of a *read* simultaneously. This makes anchoring very effective – a divide and conquer technique which entails chunking the *read* (at an anchored base position) to shorter substrings and attempting mapping on each chunk simultaneously. Thereby, problematic chunk(s) (and hence the entire *read*) simply follow the alignment dictated by the less-corrupted chunks, which by construction renders the most accurate mapping under noise. Numerous prevalent *read mapping* algorithms [14] therefore use anchoring-based techniques for complex corruptions.

## 2.3 Hardware Organization

Fig. 4 provides the structural organization. GeNVom pipeline comprises two major units: Filter Unit (FilterU) and Match Unit (MatchU). Each *query* from the dataset to be mapped streams into the (first stage of the) GeNVom pipeline (i.e., FilterU) over the *input queue*. Once the mapping completes, the outcome streams out of the (last stage of the) GeNVom

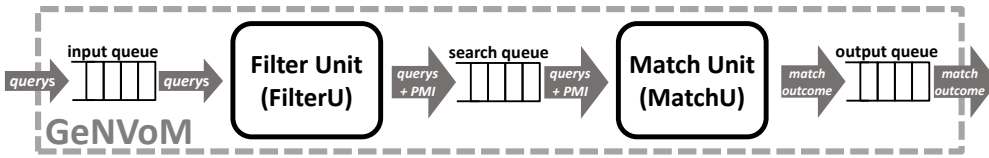


Figure 4: Structural organization.

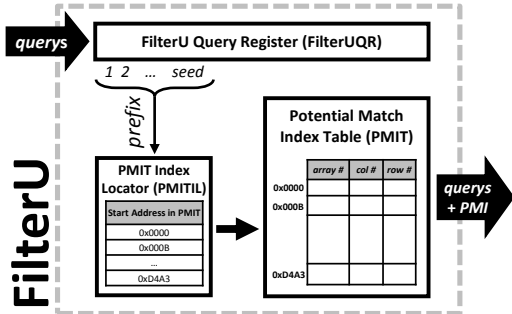


Figure 5: Filter Unit (FilterU).

pipeline (i.e., MatchU) over the *output queue*. Non-volatile TCAM arrays (which feature GenVoM’s novel similarity matching mechanism) within MatchU keep the entire *reference*.

Input and output queues handle the communication to the outside world, by retrieving *queries* on the input end, and upon completion of the mapping, by providing the indices of the most *similar* sub-sequences of the *reference* to each *query*, on the output end.

FilterU filters (indices of) sub-sequences of the *reference* which are more likely to result in a match to the incoming *query*, by examining sub-sequences of the incoming *query* itself. We call these indices *potentially matching indices*, PMI. FilterU feeds the MatchU with a stream of  $\langle \text{PMI}, \text{query} \rangle$  tuples over the *search queue*. MatchU in turn conducts the search by only considering PMI of the *reference*. In this manner, GenVoM prunes the search space.

The input queue feeds the GenVoM pipeline with the *queries* to be mapped to the *reference*. The *query* dataset resides in memory. GenVoM initiates the streaming of the *queries* into the memory-mapped input queue over a Direct Memory Access (DMA) request. The input queue in turn sends the *queries* to FilterU for search space pruning before the search takes place. Finally, for each *query*, once the mapping completes, the output queue collects from MatchU the indices of the sub-sequence of the *reference* featuring the most similar match to the *query*. The output queue is memory-mapped, too. So, GenVoM writes back these indices to a dedicated memory location, over DMA.

In the following, we will detail the steps for *query* processing in each unit in case of a match. If no sub-sequence of the *reference* matches the input *query*, no mapping takes place, and GenVoM updates a dedicated flag at the memory address to hold the result. GenVoM can detect such failed mapping attempts during processing at FilterU or at MatchU.

### 2.3.1 Filter Unit (FilterU)

Fig. 5 provides the structural organization of FilterU, which serves the compaction of the search space for each *query* to be mapped to the *reference*, as follows: We will refer to each sub-sequence of length *seed* as a *prefix*, where *seed* represents a design parameter and assumes a much lower value than the *query* length. As each *prefix* is a string of characters from

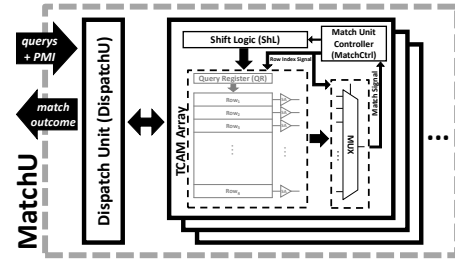


Figure 6: Match Unit (MatchU)

the 4-character alphabet {A, G, C, T}, a *prefix* of length *seed* can take  $4^{\text{seed}}$  different forms. Considering the size of the problem, the *reference* is likely to occupy multiple TCAM arrays. FilterU relies on a pre-processing step which entails identifying each *prefix* of length *seed* in the *reference*, and recording the TCAM array, column and row number of the corresponding occurrence. *Potential Match Index Table* PMIT keeps this information.

However, as the same *prefix* may occur multiple times along the *reference* string, PMIT may contain multiple entries for the very same *prefix*. Therefore, FilterU has another table called *PMIT Index Locator* (PMITIL) for bookkeeping. PMITIL serves as a dictionary of  $4^{\text{seed}}$  entries, considering all possible  $4^{\text{seed}}$  values of the (*seed*-long) *prefix*. Each PMITIL entry refers to a specific *prefix* value, and keeps the start address in PMIT where the TCAM indices for the corresponding occurrence of the *prefix* (along the *reference*) reside. As PMIT is organized to keep multiple occurrences (along the *reference*) of the same *prefix* consecutively, it suffices to keep per PMITIL entry just the start address (in the PMIT) for the first occurrence. The end address in this case simply corresponds to the start address stored in the next PMITIL entry.

PMIT and PMITIL generation constitutes a pre-processing step which GenVoM needs to perform only once, offline, for each *reference*, before *read mapping* starts. As *read mapping* entails mapping a large number short *reads* to a given *reference* of the same species, this overhead does not apply to runtime, and is easy to amortize.

Upon receipt of a new *query* from the head of the input queue, FilterU uses the first *seed* bases of the *query* as the *prefix* to consult PMITIL, and subsequently, PMIT. FilterU keeps the *query* being processed in the FilterU Query Register (FilterUQR) as filtering is in progress. If there is a match in the PMI tables, FilterU first broadcasts the *query* being processed to all TCAM arrays. Then, it sends the corresponding TCAM array, column and row number (i.e., the Potential Match Indices, PMIs) to MatchU, over the *search queue*. We will refer to these TCAM coordinates as *array#*, *col#*, and *row#*, respectively.

### 2.3.2 Match Unit (MatchU)

Fig. 6 provides the structural organization of MatchU, which orchestrates search. MatchU features the *Dispatch Unit* (DispatchU) and non-volatile TCAM arrays capable of similarity

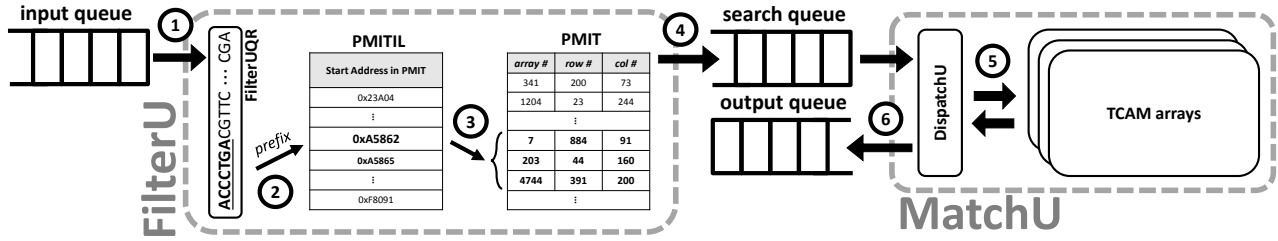


Figure 7: Life-cycle of a query in GeNVoM.

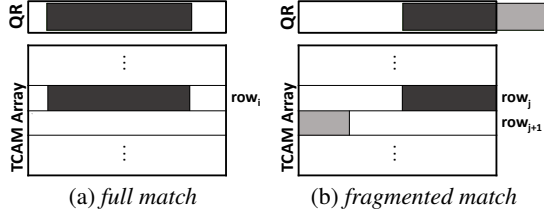


Figure 8: Full (a) and fragmented (b) TCAM match.

search under NGS or genomic variation induced noise. DispatchU acts as a scheduler for TCAM search. For each input query to be mapped to the reference, DispatchU collects the TCAM array#, col# and row#, as extracted from the PMIT in FilterU, to initiate the targeted search.

The input query stays in the Query Register (QR) of the TCAM array array# during TCAM access. Shift Logic (ShL) in TCAM array array# in turn first aligns the prefix of length seed of the query with the seed-long (matching) sub-sequence of the reference residing (in array array#) in row row#, starting from column col#. To this end, ShL shifts query bits in QR and inserts Xs accordingly. Match Unit Controller (MatchCtrl) orchestrates this operation. Once alignment completes, MatchCtrl activates the row row# for search. Once the search completes, MatchCtrl provides DispatchU with the indices of the reference which demarcate the most similar sub-sequence to the entire query. DispatchU then forwards these indices to the output queue.

Fig. 8 depicts two different match scenarios: In Fig. 8a, the query (shown in dark shade within QR, white space corresponding to Xs for padding) matches a sub-sequence of the reference which is entirely stored in a single row of the array. We call this scenario a full match. On the other hand, in Fig. 8b, the query matches a sub-sequence of the reference which is stored in two consecutive rows of the array. We call this scenario a fragmented match. Fragmentation can happen at both ends of the query. For example, in Fig. 8b, the first portion of the query (shown in darker shade) matches the end of row j, while the rest (shown in lighter shade) matches the beginning of the next row, row j+1. MatchCtrl needs to address such fragmentation as GeNVoM lays out the character string representing the reference in two dimensions in each array consecutively.

Conventional TCAM can only detect full match. Handling fragmented match requires extra logic. By default, the TCAM array would select the longest sub-sequence l of the reference matching the input query if a full match is not the case, where l occupies an entire row. The darker-shade region in Fig. 8b corresponds to such l. As l may be aligned to either the beginning (Fig. 8b) or the end of the query, MatchCtrl has to additionally check the next or the previous row, respectively, for a match to the unmatched portion of the query. We call the first case a fragmented tail match; the second, a fragmented

head match. In case of a fragmented match, search in the TCAM array takes two steps. As a fragmented match may also happen at TCAM array boundaries, each array's last row keeps the contents of the first row of the next array in sequence.

### 2.3.3 Putting It All Together

Fig. 7 summarizes the 6 steps in mapping a query to the reference: First, FilterU retrieves a new query from the head of the input queue at step ①. In this case seed=7 (bases) with the corresponding 7-base prefix of the query underlined. Then, at step ②, FilterU locates the entry for the 7-base prefix of ACCCTGA in PMITIL, and extracts the corresponding PMIT address(es). Next, at step ③, FilterU retrieves TCAM array, column, and row numbers (i.e., array#, col#, and row#; for targeted search in MatchU) for the sub-sequences of the reference which match the prefix ACCCTGA, from the PMIT addresses collected at step ②. Finally, FilterU sends the query along with array#, col#, and row# to MatchU over the search queue at step ④. At step ⑤, DispatchU initiates search in TCAM array array#, at row# and col#, and collects the match outcome. At step ⑥, MatchU sends the match outcome to the output queue.

## 3. GeNVoM: MICROSCOPIC VIEW

### 3.1 Search Space Pruning

In order to prune the search space, GeNVoM first locates sub-sequences of the reference matching the seed-long prefix of the query in FilterU (Section 2.3). seed represents a key GeNVoM design parameter which dictates not only the storage complexity, but also the degree of search space pruning, which in turn determines GeNVoM's throughput performance and energy efficiency.

PMITIL grows with  $4^{seed}$ , therefore, the larger the seed, the higher becomes the storage complexity. However, a larger seed is more likely to result in a lower number of prefix matches in the PMI tables, and hence, a lower number of targeted searches in the MatchU. In either case, the seed value remains much less than the expected length of the query.

PMIT can have at most as many entries as the total number of seed long sub-sequences contained within the reference. This practically translates into the length of the reference, as a prefix can start from each base position of the reference onward. As PMIT is organized to keep multiple occurrences of the same prefix consecutively, each PMITIL entry just keeps the start address in the PMIT for the first occurrence. PMIT, on the other hand, has to keep the <TCAM array number, column number, row number> tuple for each prefix match. If the reference is the human genome, PMIT would have approximately 3Giga entries. As we will detail in Section 4.2, 32 bits suffice to store each <TCAM array number, column

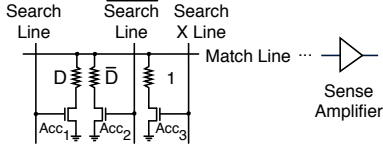


Figure 9: Resistive TCAM cell [6].

number, row number> tuple per PMIT entry; and 32 bits, each <PMIT start address> per PMITIL entry.

PMIT keeps the entries corresponding to the very same *prefix* always at consecutive addresses, and re-orders such entries further to have all entries pointing to the same TCAM array reside at consecutive addresses. GeNVom processes multiple PMIT matches per *prefix* in this consecutive order. Under such re-ordering, communicating a list of PMIs and performing search in the array happen in a pipelined fashion. This masks communication latency and consequently, can improve throughput performance significantly.

### 3.2 Data Representation

Each input *query* and the *reference* itself represent character strings over the alphabet {A, G, C, T}. Conventional bioinformatics formats such as FASTA [15] encode each letter from such alphabets of bases by single-letter ASCII codes. However, TCAM arrays conduct the search at bit granularity. Therefore, GeNVom needs to translate *base character* mismatches to *bit* mismatches. To this end, GeNVom adopts an encoding which renders the very same number of mismatched bits for a mismatch between any two base characters. This would not be the case, if we encoded each base character in {A, G, C, T} by simply using 2 bits: a base-mismatch would sometimes cause a 2-bit mismatch (e.g., when comparing ‘01’ to ‘10’); other times, a single-bit mismatch (e.g., when comparing ‘00’ to ‘10’). GeNVom’s encoding instead uses 3 bits per base character, where any two 3-bit code-words differ by exactly 2 bits, such as {111, 100, 010, 001}. Thereby GeNVom guarantees that exactly 2 bits would mismatch for any base character mismatch.

### 3.3 Similarity Search

Fig. 9 depicts a representative resistive TCAM cell. The two resistors attached to the access transistors  $Acc_1$  and  $Acc_2$ , respectively, carry the data bit value  $D$  and its complement  $\bar{D}$ . The high (low) resistance value  $R_{high}$  ( $R_{low}$ ) encodes logic 1 (0). The third resistor attached to  $Acc_3$  is hardwired to logic 1, hence its resistance remains constant at  $R_{high}$ .

To search for logic 0, *Search Line* ( $SL$ ) is set to 0, and its complement  $\bar{SL}$  to 1, such that  $Acc_2$  turns on;  $Acc_1$  off. Thereby only the resistor carrying  $\bar{D}$ ,  $R$ , gets connected to the *Match Line* ( $ML$ ). If the cell content was 0, i.e.,  $D = 0$  and  $\bar{D} = 1$ , there would be a match, and  $R = R_{high}$  applies. Otherwise, if the cell content was 1, i.e.,  $D = 1$  and  $\bar{D} = 0$ , there would be a mismatch, and  $R = R_{low}$  applies. A symmetric discussion holds for searching for logic 1. On a per TCAM cell basis,  $R_{high}$  connected to  $ML$  indicates a match,  $R_{low}$ , a mismatch. To search for X, both  $SL$  and  $\bar{SL}$  are set to 0, and *Search X Line* to 1, such that only the hard-wired  $R_{high}$  attached to  $Acc_3$  is connected to  $ML$ . This is how search for X always renders a match, independent of the value of  $D$ . Each cell within each row contributes to the effective resistance connected to  $ML$ ,  $R_{eff}$ , by  $R_{high}$  ( $R_{low}$ ) on a match (mismatch). The *Sense Amplifier* SA (connected to the  $ML$ ) in each row signals a (mis)match for the entire row depending

on the value of  $R_{eff}$ . SA would only signal a row-wide match, if all cells match, i.e., if each cell contributes to  $R_{eff}$  by  $R_{high}$ . Let us call the  $R_{eff}$  in this case  $R_{row-wide-match}$ . SA would signal a row-wide mismatch if at least one cell mismatches, i.e., contributes to  $R_{eff}$  by  $R_{low}$ . The value of  $R_{eff}$  in this case evolves with the number of cell mismatches, and assumes the closest value to  $R_{row-wide-match}$  under a single-cell (bit) mismatch. The contents of the TCAM query register directly correspond to the values on the search lines.

In a TCAM array based on the cell from Fig. 9, unless all bits within a row match, SA always signals a mismatch for the entire row. However, as explained in Sect. 2.1, a matching *query* may indeed have a few bases different from the corresponding sub-sequence of the *reference*, due to NGS or genomic variation induced noise. To resolve this discrepancy, GeNVom deploys tunable SAs which associate a wider  $R_{eff}$  range with a row-wide match. We can tune these SAs to signal a row-wide match when less than a given number  $t$  of bits mismatch, which translates into less than  $t R_{low}$ s connected to  $ML$ . We will refer to  $t$  as the *tolerance*, which represents an adjustable design parameter.

The gap between  $R_{eff}$  levels corresponding to different number of mismatching bits decreases as the number of mismatching bits grows, complicating SA design. At the same time, due to PVT (Process, Voltage, Temperature) variations, individual TCAM cell resistance levels may notably deviate from nominal  $R_{high}$  or  $R_{low}$ , leading to divergence of such  $R_{eff}$  levels from their expected values. In Sect. 4.4, we will detail how GeNVom tunes the SAs in a variation-aware fashion.

Using GeNVom’s 3-bit (per base) encoding (Sect. 3.2), any single-base mismatch results in exactly 2-bit mismatches. Under the more intuitive 2-bit encoding, on the other hand, a base-mismatch sometimes causes 2-bit mismatches; other times, a single bit mismatch, further complicating the configuration of *tolerance*.

### 3.4 Hierarchical Multi-Phase Search

Our focus so far was on the very basics of GeNVom’s mapping mechanism. We will next look into the mapping accuracy, specifically, under what circumstances GeNVom may not be able to map a given *query* to the respective *reference*, which in fact was *similar enough*. In the following, we will refer to such cases as *missed mappings*. NGS imperfections (i.e., read errors) and genomic variations complicate mapping, and thereby can lead to misses.

As explained in Sect. 2.1, GeNVom is designed to operate under all prevalent manifestations of read errors and genomic variations. To this end, GeNVom employs multi-phase hierarchical mapping. Fig. 10 provides an overview. Each phase acts as a filtering layer for the subsequent phase, which in turn performs more complex mapping. *More complex mapping* entails re-attempting by considering *more complex manifestations* of read errors/genomic variations than the predecessor phase did. In this manner, each phase re-attempts mapping only for the subset of *queries* that the previous phase missed to map.

If the mapping in a phase fails, MatchU raises the *Missed-Map* signal. GeNVom in turn feeds *Missed-Map* back to FilterU, to trigger more complex mapping attempts in the subsequent phase(s).

**Phase 1** attempts a basic mapping in the TCAM arrays, assuming that a reverse complement (Sect. 2.1) is not the case.

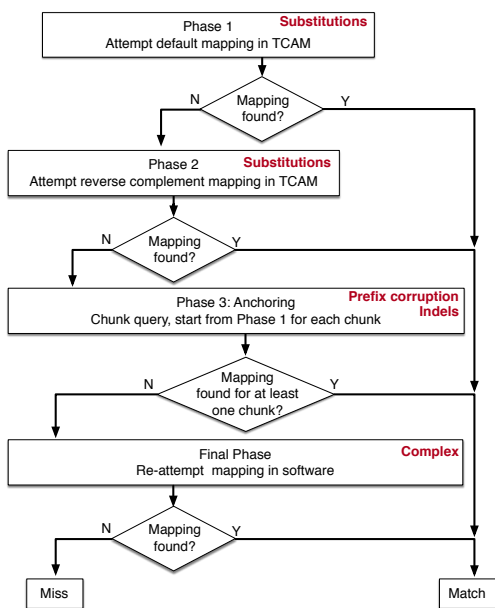


Figure 10: GeNVom’s hierarchical multi-phase search flow.

In Phase 1, FilterU and MatchU closely follow the steps detailed in Sect. 2.3. GeNVom TCAM search, by construction, can effectively identify similarity under base substitutions, which represent the common case per Fig. 3. Phase 1 can miss a mapping under three cases:

- (i) **Reverse complement:** the *query* is a *read* sequenced in reverse order. The probability for this case,  $P(i)$ , is approximately 50%.
- (ii) **Prefix corruption:** the *query*’s *seed-long prefix* (used for search space pruning in FilterU) has substitutions or indels. A corrupted *prefix* may lead to ill-addressed search requests, i.e., FilterU sending incorrect PMIs to MatchU. If the probability of having a corruption in a given base location is  $P(loc)$ , the probability for this case,  $P(ii)$ , becomes  $1 - (1 - P(loc))^{seed}$ . We can estimate  $P(loc)$  by adding a typical read error rate of 0.1% [7] to an average genome variation rate of 0.1% [8, 9, 10]. Using this estimate, for a representative *seed* value of 15 (Sect. 4),  $P(ii)$  barely reaches 3.0%.
- (iii) **Indels:** the *query* contains indels, anywhere. The most common indels are short indels induced by genome variations. Let  $P(indel)$  be the probability of a short indel, and  $len$ , the length of the *query*. Then,  $P(iii) = 1 - (1 - P(indel))^{len}$  applies. While there is no consensus on  $P(indel)$ , 0.01% represents a conservative estimate [8, 16], which renders  $P(iii) \approx 1.5\%$  for a typical *query* length of 150 [1].

**Phase 2** handles missed mappings due to reverse complements. After getting *Missed-Map* from MatchU (at the end of Phase 1), FilterU immediately sends PMIs corresponding to the reverse complement of the *query* to MatchU. To accelerate processing, MatchU employs an extra register inside the Shift Logic, which keeps the reverse complement of the *query* in addition to the original. MatchU copies the reverse complement in this register at the time it gets the original *query* (during Phase 1). Therefore, upon receipt of *Missed-Map*, FilterU does not need to broadcast the reverse complement separately, but only the PMIs for the reverse complement



Figure 11: An example of anchoring.

(which FilterU simply extracts by consulting the PMI tables with the *seed-long prefix* of the reverse complement.)

**Phase 3** handles missed mappings due to *prefix* corruptions and indels, by adapting *anchoring* [14]. This phase processes all *query*s which Phase 2 was not able to map. Phase 3 first anchors the *query* in the middle to chunk the *query* uniformly into two. Then, each chunk separately goes through Phase 1, and if necessary, through Phase 2. Unless Phase 1 (or Phase 2, as need be) manages to map at least one of the two chunks to the *reference*, Phase 3 is considered to miss the mapping.

Fig. 11 depicts an example where Phase 3 maps a *read* which Phase 1 fails to map due to prefix corruption. The top row depicts the relevant portion of the *reference*. The second and third rows show the corresponding *read*, with pointers to the matching outcome at Phase 1 and 3, respectively. The alignment of the *read* w.r.t. the *reference* reflects the ideal alignment (which renders the most similar mapping). The shaded portion corresponds to the *prefix* (of length 4 in this case). The *read* and *prefix* lengths are not representative, but ease illustration. Phase 1 fails to identify this alignment due to the single base corruption (C→A) in the third base of the *prefix*. Phase 2 is of not much help either, as a reverse complement is not the case. Phase 3 comes to rescue, by chunking, i.e., *anchoring* the *read* in the middle, and attempting mapping for each half. The mapping of the first half still fails in this case, due to the very same corruption in the *prefix*. The *prefix* of the second half (i.e., CGAT), however, is not corrupted, and GeNVom TCAM arrays can easily handle the single base mismatch in this half, which renders the correct alignment as a result – simply following the alignment dictated by the second half for the entire *read*.

Similar to this example, the proof-of-concept GeNVom design adapts 2-way chunking for anchoring, where multi-way (and not necessarily uniform) chunking can further help reduce the number of missed mappings. Anchoring essentially is a *divide and conquer* method. The key insight is that corruptions to lead to missed mappings are much less likely to occur in all of the shorter chunks simultaneously. In Sect. 5.2, we will demonstrate how anchoring can improve mapping accuracy significantly.

Phase 3 can miss a mapping under the very same two conditions as Phase 1 (namely *prefix* corruptions and indels anywhere; cases (ii) and (iii)), but only if these conditions apply to both of the chunks under *anchoring*. Under uniform two-way chunking, a typical *query* length of 150 bases renders a chunk length of 75, for which  $P(ii)$  and  $P(iii)$  become 3.0% and 1.0%, respectively. Hence, the probability to miss the mapping of a chunk would be approximately 4.0%. As Phase 3 can miss a mapping only by missing both chunks, the probability of missing a mapping in Phase 3 becomes approximately  $(4.0\%)^2 = 0.16\%$ .

By construction, anchoring can also help with more complex scenarios than indels or prefix corruptions, including long-indels, gaps, base duplications or inversions, as long as one half of the affected *query*s is still mappable by GeNVom. While anchoring reduces the miss probability significantly,

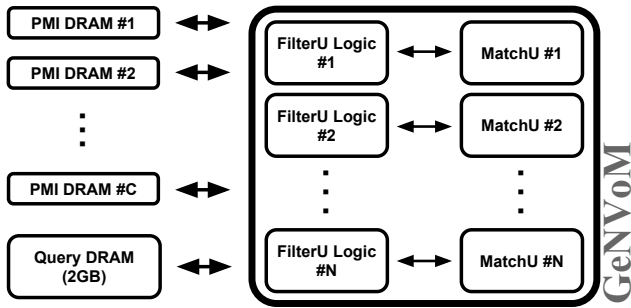


Figure 12: Organization of a single GeNVomcard.

Phase 3 may still miss mappings due to rare complex variations. To map such problematic *queries*, GeNVom can always be paired with sophisticated software algorithms.

## 4. EVALUATION SETUP

### 4.1 System-level Characterization

Without loss of generality, all components of the proof-of-concept GeNVom design reside in a single card attached to the PCIe bus. The host loads the *reference*, PMIT, and PMITIL tables to the GeNVom card before mapping starts.

We evaluate GeNVom using  $N$  different FilterUs and MatchUs to increase parallelism, as shown in Fig. 12. Each MatchU stores  $1/N$  of the reference genome. Therefore, having multiple MatchUs does not need extra TCAM space, but needs more NOC resources to feed all MatchUs in parallel. On the other hand, each FilterU is dedicated to a single MatchU, covering potential matching indices corresponding to the part of the genome stored in that MatchU. Hence, we divide PMIT table, as well, into smaller banks each corresponding to a FilterU, and a MatchU consequently. Having multiple PMIT banks for each FilterU only needs chunking, and no extra space. Besides, we need a separate PMITIL table for each PMIT bank. As discussed in Section 2.3, size of PMITIL tables depends on the *seed* only, not the size of PMIT. Then, having  $N$  FilterUs and MatchUs increases the space needed to store PMITILs by a factor of  $N$ .

A total on-card DRAM space of size  $M$  Giga bytes stores all PMIT and PMITIL tables. The  $M$  Giga bytes of memory is connected to GeNVom via  $C$  channels, to increase bandwidth of loading PMIs to meet the needs of FilterUs. A dedicated memory of 2 Giga bytes is used to store the queries. Each GeNVom design is characterized by the four parameters,  $M$ ,  $C$ ,  $L$ , and  $N$  in the evaluation section, where  $L$  represents the *seed* value. We sweep these 4 parameters and quantify throughput and energy-efficiency.

GeNVom relies on a GPU kernel (based on [17]) to reformat the match outcome of mapped *queries*, i.e., to find different SAM format fields such as CIGAR and MAPQ. We run the kernel on an NVIDIA K40 node in parallel, where it processes mapped *queries* in a pipe-lined manner periodically. This significantly reduces throughput overhead of running the GPU kernel, while we quantify its energy-efficiency implications by real measurements (similar to Section 4.6).

We use a modified version of Ramulator [18] for simulation. While the default Ramulator can model accesses to the DRAM chips, we implement intra-card interactions during search, control logic and network related operations. We model LPDDR4-4266 DRAM memory to store PMIT, PMI-TIL tables, and the queries. We use DRAMPower [19] to

	Size (GB)					
<i>seed</i>	10	11	12	13	14	15
PMITIL	0.004	0.017	0.067	0.268	1.074	4.295

Table 1: PMITIL table capacity as a function of *seed*.

estimate DRAM power consumption. DRAMPower does not simulate LPDDR4. Therefore, we conservatively estimate DRAM power using DRAMPower’s LPDDR3 model.

### 4.2 PMI Table Generation

As explained in Section 3.1, PMIT keeps an entry for each possible *seed*-long *prefix* contained within the *reference*. In other words, PMIT keeps an entry for each possible base position in the *reference* to demarcate the start of a *seed*-long *prefix*. Therefore, PMIT capacity becomes practically independent of the *seed* for feasible *seed* values. Allocating an entry for each possible base position in the *reference*, a tight-enough upper bound for PMIT capacity for the human genome used as the *reference* for evaluation (Section 4.5) is approximately 11.4GB, independent of the *seed*. As explained in Section 4.1, having  $N$  PMI banks does not need extra space.

On the other hand, PMITIL contains  $4^{seed}$  entries. We evaluate GeNVom considering different *seed* values. Table 1 captures PMITIL capacity for practical *seed* values ranging from 10 to 15. PMIT size and  $N \times$  PMITIL size together,  $M$ , determine the DRAM space requirement of the proof-of-concept GeNVom implementation.

### 4.3 Circuit-level Characterization

The proof-of-concept GeNVom implementation uses Phase Change Memory (PCM) as the resistive memory technology for TCAM arrays, which features a relatively high  $R_{high}$  to  $R_{low}$  ratio: 11.5 on average [20]. A higher  $R_{high}$  to  $R_{low}$  ratio eases sensing (i.e., distinguishing between matches and mismatches as explained in Section 3.3), therefore, enables arrays with longer rows. GeNVom’s TCAM arrays are similar to the most energy-efficient design from Guo et al. [6], which corresponds to a  $1K \times 1K$ bit configuration.

We synthesize logic circuits by Synopsys Design Compiler vH2013.12 using the FreePDK45 library [21]. To match the technology of our baselines for comparison (Section 4.6), we scale the outcome from 45nm to 28nm using ITRS projections [22]. GeNVom’s logic operates at 1GHz. A single search operation takes 1ns to complete, while consuming 0.1nJ of energy. For TCAM array area estimates, we scale numbers from [6] to 28nm. We use ORION2.0 [23] to model the network. Intra-DIMM H-tree network operates at 1GHz, while each hop (1 router + link) consumes 3.83mW.

### 4.4 Similarity Matching Specification

GeNVom adopts the Voltage Latch Sense Amplifier (VLSA) design from [24] to implement tunable sensing as explained in Section 3.3. We simulate VLSA in HSPICE v2015.06 using the FreePDK45 [21] library. VLSA’s threshold voltage sets the boundary between the ranges of the effective resistance,  $R_{eff}$ , values the SA perceives as a (row-wide) match or a mismatch. We configure VLSA’s threshold voltage to account for potential fluctuation in  $R_{high}$  and  $R_{low}$  values due to PVT variations.

#### 4.4.1 Setting the sensing threshold

We conduct a Monte Carlo analysis using the (variation-

afflicted)  $R_{high}$  and  $R_{low}$  distributions from IBM [20], extracted from measured data:  $\mu(R_{high}) = 243.8K\Omega$ ,  $\sigma(R_{high}) = 50.9K\Omega$ ,  $\mu(R_{low}) = 21.2K\Omega$ , and  $\sigma(R_{low}) = 2.5K\Omega$ .  $\mu$  and  $\sigma$  represent the mean and the standard deviation. Considering a row size of 1Kbits, we find  $R_{eff}$  for 1M sample scenarios each corresponding to a different number of base mismatches. Using the resulting  $R_{eff}$  distribution, and capping the maximum number of base mismatches that are permitted to pass as a match (i.e., the *tolerance* as explained in Section 3.3), we set SA’s sensing threshold in a variation-aware manner, in a way to make sure that SA will not produce false negatives. In other words, we make sure that SA will never signal a mismatch, when query is similar-enough.

#### 4.4.2 Sensing Accuracy

As explained in Section 3.3, under PVT variations, sense amplifiers may trigger a (row-wide) match in case of an actual (row-wide) mismatch. For each such case, the number of base mismatches remains higher than the preset *tolerance* value. In the following, we will refer to this difference in the number of base mismatches with respect to the *tolerance* as *overshoot*. These cases are not necessarily errors, and rather translate into a *query* of less similarity than expected being matched to a sub-sequence of the *reference*. Therefore, as long as the overshoot (in terms of base mismatches) with respect to the anticipated *tolerance* remains bounded, each such case can easily pass as a *less similar match* (which in fact can be an actual match where the input *query* was significantly corrupted). Monte Carlo analysis from Section 4.4.1 shows that for different representative *tolerance* values used in Section 5, overshoot is usually less than 3, with probability of an overshoot of size 3 or larger barely reaching 0.05%. We quantify the impact of SA’s inaccuracy on GeNVom’s overall accuracy in Section 5.2.

### 4.5 Input Dataset

We use a real human genome, g1k\_v37, from the 1000 genomes project [25] as the *reference* genome; and 20 million 100-base long real *reads* from NA12878 [26] as a *query* dataset. For mapping accuracy analysis, we further generate 20 million more *queries* using 100-base long randomly picked sub-sequences from this *reference*, which we corrupt considering a read error probability of 0.1% (to mimic modern Illumina platforms), a single substitution<sup>1</sup> probability of 0.09%, and a short indel probability of 0.009% []. For a fair comparison (not to favor GeNVom) we choose the number of *queries* to have the *reference* + *queries* fit into the main memory of the GPU, such that the GPU does not suffer from extra energy-hungry data communication. We also limit the evaluation to a single GeNVom card to keep the resource utilization comparable to the baselines.

### 4.6 Baseline for Comparison

As a comparison baselines, we pick a highly optimized GPU implementation of the popular BWA algorithm, SOAP3-dp [12], and a short-read aligner hardware accelerator, GenAx [27]. A pure software-based implementation of GeNVom is orders of magnitude slower than SOAP3-dp. We evaluate the throughput performance and power consumption of SOAP3-dp on an NVIDIA Tesla K40 GPU. We measure the power

<sup>1</sup>i.e., single-nucleotide polymorphism, SNP, the dominant type of substitutions induced by genomic variations

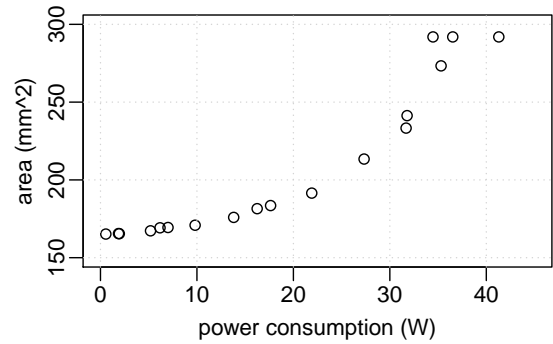


Figure 13: GeNVom’s area and power consumption for different evaluated designs.

consumption of the GPU using NVIDIA-SMI (System Management Interface) command. We use the same *reference* and *query* dataset (Section 4.5) as GeNVom as inputs. We compare GeNVom against two different configurations of SOAP3-dp: The first one, SOAP<sub>SUB</sub>, only handles substitutions; the second one, SOAP<sub>ALL</sub>, captures all prevalent manifestations of read errors and genomic variations.

### 4.7 Design Space Exploration

We sweep  $M$ ,  $C$ ,  $N$ , and  $L$  in the evaluation section to find the highest throughput design,  $GeNVom_{Perf}$ , the most energy-efficient design,  $GeNVom_{Energy}$ , and a design optimized for both,  $GeNVom_{Optim}$ . We sweep  $M$  from 16GB to 128GB, and  $L$  from 10 to 15. For each  $L$ , we find the maximum  $N$  where PMIT size and  $N \times PMITIL$  size fits in the given  $M$  budget. Besides, we cap  $N$  at 512, to limit  $C$ , number of LPDDR4-4266 channels needed to feed PMIs to FilterUs, at 64. Fig 13 depicts how the ranges of area and power consumption of GeNVom looks like for different evaluated designs with different  $M$ ,  $C$ ,  $N$ , and  $L$  parameters.

## 5. EVALUATION

### 5.1 Throughput Performance and Energy

Larger *seed* values prune the search space more, resulting in a progressively lower number of search operations in processing each *query*. Increasing  $L$  from 10 to 15 decreases average number of search operations per query from 30.2K to 4.6K. On the other hand for a given  $M$  budget, lower  $L$  leads to larger  $N$  values, which consequently increases parallelism level of GeNVom. Therefore, we need to sweep  $L$  for different  $M$  DRAM budgets to find the optimum  $L$  value.

Fig. 14a depicts the throughput performance of GeNVom. Y-axis represents the number of *queries* mapped per second. X-axis shows the number of FilterUs/MatchUs used,  $N$ . The two red horizontal lines correspond to the throughput of the two baselines, SOAP3-dp and GenAx. Each line corresponds to a different  $M$  budget. Each point belongs to a different  $L$ . We do not include the  $L$  values which violate the cap of  $N$ , 512.

As Fig. 14a shows, starting from  $L$  of 15 (on the left side), decreasing  $L$  increases  $N$ , and consequently increases throughput. However, as  $L$  goes lower than 12, the extra number of searches dominates the benefits of a larger  $N$ , leading to slow-down in performance. Besides, we see that having a larger  $M$  budget improves the overall throughput. While most points are above both baseline lines, the fastest design,  $GeNVom_{Perf}$ , gives up to  $113.5 \times$  speed-up over SOAP3-dp,

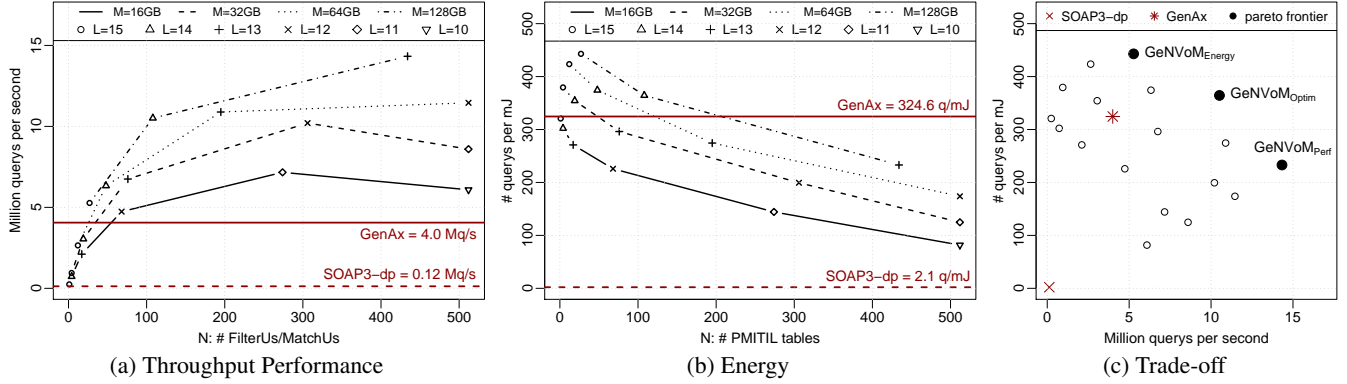


Figure 14: Throughput performance and energy consumption.

and  $3.6\times$  over GenAx, for  $M = 128GB$ ,  $L = 13$ ,  $C = 55$ , and  $N = 434$ .  $GeNVOM_{Perf}$  consumes 35.3 Watts of power on average, and  $273.3\text{ mm}^2$  of area.

Fig. 14b demonstrates the energy efficiency of GeNVom. Y-axis represents the number of *queries* mapped per Millie Joule of energy (q/mJ). X-axis shows the number of FilterUs/MatchUs used,  $N$ . The two red lines correspond to the q/mJ rate of the two baselines. Similar to the throughput figure, each line represents a different  $M$  budget, and each point shows a different  $L$ .

As we see in Fig. 14b, energy efficiency worsens for smaller  $L$ s, since number of searches increases for smaller  $L$ s, and at the same time,  $N$  grows and consequently we see more power consumption in FilterUs, MatchUs, and NOCs. GeNVom outperforms SOAP3-dp in energy-efficiency for all evaluated parameters, while still many designs outperform GenAx. The most energy efficient design,  $GeNVOM_{Energy}$ , mapping 442.9 queries per Millie Joule, corresponds to  $M = 128GB$ ,  $L = 15$ ,  $C = 4$ , and  $N = 27$ .  $GeNVOM_{Energy}$  outperforms energy-efficiency of SOAP3-dp by  $210.9\times$  and GenAx by  $1.36\times$ , while consuming 5.2 Watts of power and  $167.3\text{ mm}^2$  of area.

Finally, Fig. 14c depicts the trade-off space of throughput (x-axis) versus energy-efficiency (y-axis) for different parameters. Points closer to the top-right corner are faster and more energy efficient. The two red points represent where baselines are. All points outperform SOAP3-dp in both throughput and energy-efficiency, while a few can be both faster and more energy-efficient compared to GenAx. Besides, we see the Pareto frontier points marked with black. We pick the third design optimized for both performance and energy-efficiency,  $GeNVOM_{Optim}$ , from the Pareto-frontier points, with  $M = 128GB$ ,  $L = 14$ ,  $C = 14$ , and  $N = 108$ .  $GeNVOM_{Optim}$ , consuming 21.9 Watts of power and  $191.5\text{ mm}^2$  of area, maps 10.5 million queries per second ( $84.0\times$  faster than SOAP3-dp and  $2.6\times$  faster than GenAx) and 364.4 queries per Millie Joule ( $173.5\times$  better than SOAP3-dp and  $1.12\times$  better than GenAx). All three Pareto-frontier designs correspond to  $M = 128GB$ , which shows GeNVom benefits from larger memory space in both throughput and energy-efficiency.

Without loss of generality for  $L = 15$ , GeNVom maps 45.4% of the *queries* in Phase 1; 42.1% in Phase 2 (reverse complement); and 8.4%, in Phase 3. Specifically, in Phase 3, GeNVom maps 3.0% of the *queries* after anchoring the

first half; 2.6% after anchoring the second half; 1.8% after anchoring reverse complement of the first half; and 1.0% after anchoring reverse complement of the second half, respectively. This renders a mapping rate (i.e., the share of successfully mapped *queries* over all) of around 96.0% for GeNVom, while SOAP3-dp can map 97.4% of the *queries*.

## 5.2 Mapping Accuracy

Since we were not able to run experiments using GenAx, we compare the accuracy of GeNVom to SOAP3-dp only. Besides, SOAP3-dp outperforms accuracy of BWA [12], which has very similar accuracy to GenAx. Therefore, SOAP3-dp is expected to have better accuracy compared to GenAx. To compare the mapping accuracy of GeNVom to SOAP3-dp, we use a simulated input dataset with known expected matching indices. We differentiate between two cases: (1) the *query* is aligned to a wrong portion of the *reference*; or (2) the *query* is not aligned to any portion of the *reference*. Table 2 shows the corresponding rate of occurrence for (1) as the *Misalignment rate*; for (2), as the *Miss rate*, considering different configurations. We should note that misaligned *queries* are still mapped to a portion of the *reference*, which may be similar enough. Therefore, *misalignment rate* does not necessarily correspond to an error rate. The numbers in Table 2 reflect all errors caused by GeNVom’s prefix corruption, indel mishandling, and SA’s false positives.

	GeNVom <sub>Energy</sub>	GeNVom <sub>Optim</sub>	GeNVom <sub>Perf</sub>	SOAP3-dp
Misalignment Rate	2.94%	2.97%	2.99%	1.12%
Miss Rate	0.03%	0.03%	0.04%	0.01%
Total	2.97%	3.0%	3.03%	1.13%

Table 2: Mapping accuracy of GeNVom w.r.t. SOAP

We observe that both *misalignment rate* and *miss rate* are slightly increasing for larger  $L$  values (from GeNVom<sub>Energy</sub> to GeNVom<sub>Perf</sub>), due to higher prefix corruption probability. However, the overall accuracy of different GeNVom designs considering different  $L$  values stay in a similar range. Generally, GeNVom fails to align only around 0.03% more queries compared to SOAP3-dp, while misaligning around 1.85% more queries.

Next, we evaluate the effectiveness of GeNVom’s anchoring phase (phase 3 from Section 3.4), in improving the accuracy of mapping after the first 2 phases. Without loss of generality, GeNVom<sub>Energy</sub> fails to map 2.88% of the *queries*, after the first 2 phases, mapping normally and the reverse complement. Phase 3 of GeNVom<sub>Energy</sub>, featuring anchoring

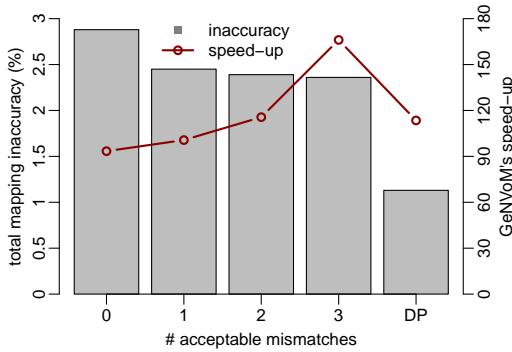


Figure 15: Impact of *tolerance* on SOAP3-dp’s accuracy and performance.

on the other hand, can map 98.6% of the *queries* that the first two phases misses (due to indels and prefix corruption), while aligning 91.2% of them to the correct index of the reference genome. This analysis demonstrates how effective multi-phase search is in improving the mapping accuracy when dealing with *queries* failed-to-map by the first two phases.

SOAP3-dp let user trade-off accuracy for higher throughput. In this mode, SOAP3-dp does not map using the dynamic programming kernel, and only relies on capturing substitution errors. User can set the accuracy level of the program by tuning the number of acceptable mismatches, which is similar to the *tolerance* level of GenVoM. Lower *tolerance* level leads to lower accuracy. At the same time, lower *tolerance* improves throughput of SOAP3-dp, since it performs lower number of search operations. On the other hand, different *tolerance* values does not affect GenVoM’s throughput noticeably, since neither FilterU’s or MatchU’s performance depend on it. More specifically, GenVoM can tune *tolerance* by only adjusting SA’s threshold, which negligibly affects TCAM search latency only.

Fig 15 depicts how SOAP3-dp’s accuracy (left y-axis) changes for different number of acceptable mismatches (x-axis). The right-most bar belongs to default SOAP3-dp parameters, which includes the dynamic programming kernel as well. The line in the figure corresponds to the speed-up of  $\text{GenVoM}_{\text{Perf}}$  versus SOAP3-dp (right y-axis). As we see, for smaller *tolerances*, SOAP3-dp becomes less accurate, and at the same time faster, which leads to lower GenVoM’s speed-up. The lowest accuracy of SOAP3-dp, 2.88% for a *tolerance* of 0, is close to accuracy of  $\text{GenVoM}_{\text{Perf}}$ . However, being 21.5% faster compared to the default SOAP3-dp, it is still  $93.4\times$  slower compared to  $\text{GenVoM}_{\text{Perf}}$ . Therefore, GenVoM outperforms even an iso-accuracy baseline by two orders of magnitude.

**A note on “acceptability”:** In a typical NGS *query* dataset, all *queries*, if concatenated back to back, would be at least  $50\times$  [28] longer than the *reference* genome. Therefore, even if we miss the mapping of a few percent of the *queries* (due to different *read* errors/genome variations), we still have plenty of *queries* to cover such missed regions of the *reference* – which would be covered by the missed *queries* were there no *read* errors/genome variations. The average number of *queries* covering any given base in the *reference* genome is called the *depth*.

Only missing all *queries* covering a specific base of the *reference* would be problematic. What is the probability for GenVoM to miss all *queries* covering a given base of the *reference*? Let the number of *queries* covering a given

base be  $Q$ , and let  $\min(Q)$  denote its minimum.  $Q$  follows a Poisson distribution [29]. For a representative *depth* of 50, the probability of having a base covered by less than 10 *queries* is  $5.2 \times 10^{-12}$ , practically negligible. Therefore, we can assume that all bases are covered by at least 10 *queries*, i.e., that  $\min(Q) = 10$ . The probability of GenVoM missing a mapping,  $P_{\text{miss}}$  is around 3.03% (Table 2). Hence, the probability of GenVoM missing all *queries* covering a base of the *reference* becomes  $P_{\text{miss}}^{\min(Q)} = 6.5 \times 10^{-16}$ , which is practically negligible.

## 6. RELATED WORK

**(Short) Read Mapping:** With no pre-processing of the *reference*, the computational complexity scales (at least) linearly with the *reference* length. Therefore, popular software implementations such as SOAP [30], Eland (part of the Illumina suite), and MAQ [31] adapt hash-based pre-processing. SOAP2 [32], Bowtie(2) [33, 34], BWA [35, 36], on the other hand, use the (more memory efficient) Burrows-Wheeler Transformation (BWT) of the *reference*. One baseline for comparison, SOAP3-dp [12], represents an open-source GPU implementation of BWA, which can also handle noise in *reads*, however, unlike GenVoM, the computational complexity depends on the *tolerance* value. Genax [27], the other baseline for comparison, is an automata-based accelerator. Similar to SOAP3-dp, computational and space complexity of GenAx depend on the *tolerance* value, unlike GenVoM. High-throughput FPGA implementations [37] also exist, at the expense of orders of magnitude higher power consumption than GenVoM. The exotic race logic based dynamic programming accelerator [38] can find the similarity between two strings corresponding to the *read* and a sub-sequence of the *reference* in approx. 120ns while consuming 1nJ. This is much slower than GenVoM, and energy grows with the third power of *read* length which can impair scalability.

Another study introduced an efficient filtering step for hash-based *read mapping* using 3D-stacked memories [39]. This covers filtering (i.e., search space pruning) only, which has a similar functionality to GenVoM’s FilterU. While the high cost of quadratic-time dynamic programming algorithms for string (i.e., *query*) matching motivated this work, GenVoM relies on much faster and more energy-efficient string matching enabled by resistive TCAM. Hence, GenVoM employs a simpler, low-latency filtering (incorporated in FilterU), which is tailored to its more efficient string matching (incorporated in MatchU). Although higher-overhead methods like [39] can prune the search space further, embedding such into GenVoM’s FilterU would be overkill, rendering FilterU the system bottleneck and diminishing the benefits from MatchU’s fast and energy-efficient similarity matching. We believe that proposals like [39] are more suitable for *long read mapping*, which represents a different problem. Besides GenAx [27], recent work also includes a BWA-based hardware accelerator featuring NVM [40], which is significantly slower than GenVoM; and very effective hardware acceleration for other significant bioinformatics algorithms [41].

**Resistive CAM Accelerators:** Guo et al. [6, 42] explore TCAM for accelerating data-intensive applications. Yavits et al. [43] propose an associative processor, which employs resistive CAM based look-up tables to implement diverse functions. Kaplan et al. [44] demonstrate how to efficiently implement Smith-Waterman algorithm (which tries to align strings of similar length) using resistive CAM based look-up

tables. Not being able to handle similarity matching under noise, neither of these are directly applicable to *read mapping*. Approximate resistive CAM is also proposed, either using exotic cells [45] (which complicates match detection, and thereby restricts the row length to at most 8 bits) or limiting the row length to 4 bits only (to find the Hamming distance, their similarity metric, robustly) [46]. While these show great potential, restricted row length hinders applicability to *read mapping* where longer (short) *reads* are emerging with NGS improvements and where TCAM search happens at row-granularity. GeNVOM adds support for approximate matches much less intrusively, by carefully tuning the sense amplifier (SA) reference voltage in a variation-aware manner, without restricting the row size. No CAM array capable of only approximate matching would be sufficient to implement an efficient *read mapping* accelerator by itself, as demonstrated in Section 2.2.

Recent representative demonstrations of resistive TCAM include a 1Gbit PCM-based CAM from IBM using IBM 90nm technology [47] with a measured search latency of 1.9ns, and two novel spintronic designs in 45nm [48], where a search takes approx. 0.6ns in 256-wide rows. GeNVOM can adapt any resistive CAM array, including these more recent proposals.

## 7. DISCUSSION & CONCLUSION

A common critical first step in a diverse set of emerging bioinformatics applications is *read mapping*, a search heavy, memory intensive approximate pattern matching problem. This suggests TCAM-based acceleration, which by definition features fast parallel in-memory search. However, the excessive energy consumption and lack of support for similarity matching under noise hinders the direct application of TCAM-based search, irrespective of volatility, where only non-volatile TCAM can accommodate the large memory footprint in an area-efficient way. This paper proposes GeNVOM, a novel *read mapping* accelerator which unlocks the throughput potential of non-volatile TCAM. GeNVOM results in up to  $113.5\times$  ( $3.6\times$ ) higher throughput while consuming up to  $210.9\times$  ( $1.36\times$ ) less energy when compared to a highly-optimized GPU (accelerator) implementation.

Currently, short (i.e., 100-200 base long) *reads* from modern Illumina NGS platforms [1] constitute more than 90% of all *reads* in the world. This dominance is unlikely to quickly change in the near future due to the progressively dropping sequencing cost of short *read* technologies, rendering them significantly more cost-efficient than the long *read* counterparts such as PacBio [49] or Oxford Nanopore [50] (where *read* lengths can exceed tens of thousands of bases). The key benefit of long *read* sequencing technologies comes from the capability of directly extracting long-range information, and not necessarily from higher accuracy. That said, many emerging recent technologies such as 10xGENOMICS [51] can obtain long-range information from short *reads*. Although it is very hard to predict the future exactly, considering practical facts such as market share and market caps, we believe that short *read* platforms will remain prevalent at least in the near future. Accordingly, GeNVOM is designed for short *read mapping*.

Short *read mapping* and long *read mapping* representing two fundamentally different problems. This is because of the difference in NGS and genomic variation induced noise manifestations. Long *reads* are subject to more frequent and

complex corruptions, which gives rise to very different algorithms for the mapping problem than short *reads*. For example, perturbation by a significant number of indels is not uncommon [52]. A very efficient hardware accelerator for long *read mapping* has also been proposed recently [53]. As such accelerators are highly optimized for long *reads* (which suffer from more complex noise manifestation), they are by construction sub-optimal for short *read mapping* (for which substitutions are dominant per Fig. 3).

The evaluated proof-of-concept implementation represents one feasible point in the rich design space of GeNVOM. 3D stacking is an option, for example, to enable even more parallelism subject to a stringent thermal budget, where the scale of the problem demands careful optimization for data communication between the memory modules and logic embedded in/near memory, which we reserve for future work.

## 8. REFERENCES

- [1] "Illumina sequencing by synthesis (SBS) technology: <https://www.illumina.com/technology/next-generation-sequencing/sequencing-technology.html>."
- [2] Z. D. Stephens, S. Y. Lee, F. Faghri, R. H. Campbell, C. Zhai, M. J. Efron, R. Iyer, M. C. Schatz, S. Sinha, and G. E. Robinson, "Big Data: Astronomical or Genomical?," *PLOS Biology*, vol. 13, July 2015.
- [3] S. Aluru and N. Jammula, "A review of hardware acceleration for computational genomics," *IEEE Design & Test*, vol. 31, no. 1, 2014.
- [4] P. Klus, S. Lam, D. Lyberg, M. S. Cheung, G. Pullan, I. McFarlane, G. S. Yeo, and B. Y. Lam, "BarraCUDA - a fast short read sequence aligner using graphics processing units," *BMC Research Notes*, vol. 5, Jan. 2012.
- [5] Y. Chen, B. Schmidt, and D. L. Maskell, "A hybrid short read mapping accelerator," *BMC Bioinformatics*, vol. 14, no. 1, 2013.
- [6] Q. Guo, X. Guo, Y. Bai, and E. Ipek, "A resistive TCAM accelerator for data-intensive computing," *IEEE International Symposium on Microarchitecture (MICRO)*, 2011.
- [7] M. Schirmer, R. D'Amore, U. Z. Ijaz, N. Hall, and C. Quince, "Illumina error profiles: resolving fine-scale variation in metagenomic sequencing data," *BMC Bioinformatics*, vol. 17, no. 1, 2016.
- [8] J. M. Mullaney, R. E. Mills, W. S. Pittard, and S. E. Devine, "Small insertions and deletions (indels) in human genomes," *Human Molecular Genetics*, vol. 19, no. R2, 2010.
- [9] S.-M. Ahn, T.-H. Kim, S. Lee, D. Kim, H. Ghang, D.-S. Kim, B.-C. Kim, S.-Y. Kim, W.-Y. Kim, C. Kim, D. Park, Y. S. Lee, S. Kim, R. Reja, S. Jho, C. G. Kim, J.-Y. Cha, K.-H. Kim, B. Lee, J. Bhak, and S.-J. Kim, "The first korean genome sequence and analysis: full genome sequencing for a socio-ethnic group," *Genome research*, vol. 19, no. 9, pp. 1622–1629, 2009.
- [10] J. Wala, P. Bandopadhyay, N. Greenwald, R. O'Rourke, T. Sharpe, C. Stewart, S. E. Schumacher, Y. Li, J. Weischenfeldt, X. Yao, C. Nusbaum, P. Campbell, M. Meyerson, C.-Z. Zhang, M. Imielinski, and R. Beroukhi, "Genome-wide detection of structural variants and indels by local assembly," *bioRxiv*, p. 105080, 2017.
- [11] R. P. Abo, M. Ducar, E. P. Garcia, A. R. Thorner, V. Rojas-Rudilla, L. Lin, L. M. Sholl, W. C. Hahn, M. Meyerson, N. I. Lindeman, P. VanHummelen, and L. E. MacConaill, "Breakmer: detection of structural variation in targeted massively parallel sequencing data using kmers," *Nucleic acids research*, vol. 43, no. 3, pp. e19–e19, 2014.
- [12] R. Luo, T. Wong, J. Zhu, L. Chi-Man, X. Zhu, E. Wu, L.-K. Lee, H. Lin, W. Zhu, D. W. Cheung, H.-F. Ting, S.-M. Yiu, S. Peng, Y. Chang, Y. Li, R. Li, and T.-W. Lam, "Soap3-dp: fast, accurate and sensitive gpu-based short read aligner," *PLoS one*, vol. 8, no. 5, 2013.
- [13] J. Leskovec, A. Rajaraman, and J. D. Ullman, *Mining of massive datasets*. Cambridge University Press, 2014.
- [14] B. Langmead, C. Trapnell, M. Pop, and S. L. Salzberg, "Ultrafast and memory-efficient alignment of short dna sequences to the human genome," *Genome biology*, vol. 10, no. 3, p. R25, 2009.
- [15] D. J. Lipman and W. R. Pearson, "Rapid and sensitive protein similarity searches," *Science*, vol. 227, no. 4693, 1985.

- [16] J. Wang, W. Wang, R. Li, Y. Li, G. Tian, L. Goodman, W. Fan, J. Zhang, J. Li, J. Zhang, Y. Guo, B. Feng, H. Li, Y. Lu, X. Fang, H. Liang, Z. Du, D. Li, Y. Zhao, and Y. Hu, "The diploid genome sequence of an asian individual," *Nature*, vol. 456, no. 7218, pp. 60–65, 2008.
- [17] "NVBIO Smith-Waterman: <https://developer.nvidia.com/nvbio/>."
- [18] Y. Kim, W. Yang, and O. Mutlu, "Ramulator: A fast and extensible dram simulator.," *Computer Architecture Letters*, vol. 15, no. 1, pp. 45–49, 2016.
- [19] K. Chandrasekar, C. Weis, Y. Li, B. Akesson, N. Wehn, and K. Goossens, "Drampower: Open-source dram power & energy estimation tool," URL: <http://www.drampower.info>, vol. 22, 2012.
- [20] H. Y. Cheng, W. C. Chien, M. BrightSky, Y. H. Ho, Y. Zhu, A. Ray, R. Bruce, W. Kim, C. W. Yeh, H. L. Lung, and C. Lam, "Novel fast-switching and high-data retention phase-change memory based on new ga-sb-ge material," in *IEEE International Electron Devices Meeting (IEDM)*, 2015.
- [21] NCSU-EDA, "FreePDK45: <https://www.eda.ncsu.edu/wiki/FreePDK45:Contents>."
- [22] L. Wilson, "International technology roadmap for semiconductors (itrs)," *Semiconductor Industry Association*, 2013.
- [23] A. B. Kahng, B. Li, L.-S. Peh, and K. Samadi, "Orion 2.0: a fast and accurate noc power and area model for early-stage design space exploration," in *Proceedings of the Design, Automation & Test in Europe (DATE)*, 2009.
- [24] M. H. Abu-Rahma, Y. Chen, W. Sy, W. L. Ong, L. Y. Ting, S. S. Yoon, M. Han, and E. Terzioglu, "Characterization of sram sense amplifier input offset for yield prediction in 28nm cmos," in *IEEE Custom Integrated Circuits Conference (CICC)*, Sept 2011.
- [25] "1000 genomes project: <ftp://ftp-trace.ncbi.nih.gov/1000genomes/ftp/technical/reference/>."
- [26] "NA12878." <ftp://ftp-trace.ncbi.nlm.nih.gov/giab/ftp/data/NA12878/>.
- [27] D. Fuijiki, A. Subramanian, T. Zhang, Y. Zheng, R. Das, D. Blaauw, and S. Narayanasamy, "GenAx: A Genome Sequencing Accelerator," *ACM/IEEE International Symposium on Computer Architecture (ISCA)*, June 2018.
- [28] S. S. Ajay, S. C. Parker, H. O. Abaan, K. V. F. Fajardo, and E. H. Margulies, "Accurate and comprehensive sequencing of personal genomes," *Genome Research*, vol. 21, no. 9, 2011.
- [29] E. S. Lander and M. S. Waterman, "Genomic mapping by fingerprinting random clones: a mathematical analysis," *Genomics*, vol. 2, no. 3, 1988.
- [30] R. Li, Y. Li, K. Kristiansen, and J. Wang, "Soap: short oligonucleotide alignment program," *Bioinformatics*, vol. 24, no. 5, 2008.
- [31] H. Li, J. Ruan, and R. Durbin, "Mapping short dna sequencing reads and calling variants using mapping quality scores," *Genome Research*, vol. 18, no. 11, 2008.
- [32] R. Li, C. Yu, Y. Li, T.-W. Lam, S.-M. Yiu, K. Kristiansen, and J. Wang, "Soap2: an improved ultrafast tool for short read alignment," *Bioinformatics*, vol. 25, no. 15, 2009.
- [33] B. Langmead, C. Trapnell, M. Pop, and S. L. Salzberg, "Ultrafast and memory-efficient alignment of short dna sequences to the human genome," *Genome Biology*, vol. 10, no. 3, 2009.
- [34] B. Langmead and S. L. Salzberg, "Fast gapped-read alignment with bowtie 2," *Nature Methods*, vol. 9, no. 4, 2012.
- [35] H. Li and R. Durbin, "Fast and accurate short read alignment with burrows-wheeler transform," *Bioinformatics*, vol. 25, no. 14, 2009.
- [36] H. Li and R. Durbin, "Fast and accurate long-read alignment with burrows-wheeler transform," *Bioinformatics*, vol. 26, no. 5, 2010.
- [37] W. Vanderbauwhede and K. Benkrid, *High-performance computing using FPGAs*. Springer, 2013.
- [38] A. Madhavan, T. Sherwood, and D. Strukov, "Race logic: A hardware acceleration for dynamic programming algorithms," *ACM/IEEE International Symposium on Computer Architecture (ISCA)*, 2014.
- [39] J. Kim, D. Senol, H. Xin, D. Lee, M. Alser, H. Hassan, O. Ergin, C. Alkan, and O. Mutlu, "Genome read in-memory (grim) filter: Fast location filtering in dna read mapping using emerging memory technologies [https://people.inf.ethz.ch/omutlu/pub/GRIM-genome-read-in-memoryfilter\\_psb17-poster.pdf](https://people.inf.ethz.ch/omutlu/pub/GRIM-genome-read-in-memoryfilter_psb17-poster.pdf)," 2017.
- [40] F. Zokaee, H. R. Zarandi, and L. Jiang, "Aligner: A Process-In-Memory Architecture for Short Read Alignment in ReRAMs," *IEEE Computer Architecture Letters*, 2018.
- [41] C. Bo, V. Dang, E. Sadredini, and K. Skadron, "Searching for potential grna off-target sites for crispr/cas9 using automata processing across different platforms," in *2018 IEEE International Symposium on High Performance Computer Architecture (HPCA)*, pp. 737–748, Feb 2018.
- [42] Q. Guo, X. Guo, R. Patel, E. Ipek, and E. G. Friedman, "AC-DIMM: associative computing with STT-MRAM," in *ACM/IEEE International Symposium on Computer Architecture (ISCA)*, June 2013.
- [43] L. Yavits, S. Kvatinisky, A. Morad, and R. Ginosar, "Resistive associative processor," *IEEE Computer Architecture Letters*, vol. 14, no. 2, 2015.
- [44] R. Kaplan, L. Yavits, R. Ginosar, and U. Weiser, "A resistive cam processing-in-storage architecture for dna sequence alignment," *IEEE Micro*, vol. 37, no. 4, pp. 20–28, 2017.
- [45] M. Imani, D. Peroni, A. Rahimi, and T. Rosing, "Resistive cam acceleration for tunable approximate computing," *IEEE Transactions on Emerging Topics in Computing*, 2017.
- [46] M. Imani, A. Rahimi, D. Kong, T. Rosing, and J. Rabaey, "Exploring hyperdimensional associative memory," *IEEE International Symposium on High Performance Computer Architecture (HPCA)*, 2017.
- [47] J. Li, R. Montoye, M. Ishii, K. Stawiasz, T. Nishida, K. Maloney, G. Ditlow, S. Lewis, T. Maffitt, R. Jordan, L. Chang, and P. Song, "1Mb 0.41  $\mu\text{m}^2$  2T-2R cell nonvolatile TCAM with two-bit encoding and clocked self-referenced sensing," in *Symposium on VLSI Circuits*, June 2013.
- [48] B. Yan, Z. Li, Y. Zhang, J. Yang, H. Li, W. Zhao, and P. C.-F. Chia, "A high-speed robust nvm-tcam design using body bias feedback," in *Great Lakes Symposium on VLSI (GVLSI)*, 2015.
- [49] "Pacific BioSciences: <http://www.pacb.com/products-and-services/pacbio-systems/>."
- [50] D. Branton, D. W. Deamer, A. Marziali, H. Bayley, S. A. Benner, T. Butler, M. Di Ventra, S. Garaj, A. Hibbs, X. Huang, S. B. Jovanovich, P. S. Krstic, S. Lindsay, X. S. Ling, C. H. Mastrangelo, A. Meller, J. S. Oliver, Y. V. Pershin, J. M. Ramsey, R. Riehn, G. V. Soni, V. Tabard-Cossa, M. Wanunu, M. Wiggin, and J. A. Schloss, "The potential and challenges of nanopore sequencing," *Nature Biotechnology*, vol. 26, no. 10, 2008.
- [51] "10xGENOMICS: <https://www.10xgenomics.com/genome/>."
- [52] M. G. Ross, C. Russ, M. Costello, A. Hollinger, N. J. Lennon, R. Hegarty, C. Nusbaum, and D. B. Jaffe, "Characterizing and measuring bias in sequence data," *Genome biology*, vol. 14, no. 5, p. R51, 2013.
- [53] Y. Turakhia, G. Bejerano, and W. J. Dally, "Darwin: A Genomics Co-processor Provides up to 15,000x acceleration on long read assembly," *ACM International Conference on Architectural Support for Programming Languages and Operating Systems (ASPLOS)*, March 2018.